RESEARCH ARTICLE

Ca^{2+} Transients in Astrocyte Fine Processes Occur Via Ca^{2+} Influx in the Adult Mouse Hippocampus

Ravi L. Rungta, Louis-Philippe Bernier, Lasse Dissing-Olesen, Christopher J. Groten, Jeffrey M. LeDue, Rebecca Ko, Sibyl Drissler, and Brian A. MacVicar

Astrocytes display complex morphologies with an array of fine extensions extending from the soma and the primary thick processes. Until the use of genetically encoded calcium indicators (GECIs) selectively expressed in astrocytes, Ca^{2+} signaling was only examined in soma and thick primary processes of astrocytes where Ca^{2+}-sensitive fluorescent dyes could be imaged. GECI imaging in astrocytes revealed a previously unsuspected pattern of spontaneous Ca^{2+} transients in fine processes that has not been observed without chronic expression of GECIs, raising potential concerns about the effects of GECI expression. Here, we perform two-photon imaging of Ca^{2+} transients in adult CA1 hippocampal astrocytes using a new single-cell patch-loading strategy to image Ca^{2+}-sensitive fluorescent dyes in the cytoplasm of fine processes. We observed that astrocyte fine processes exhibited a high frequency of spontaneous Ca^{2+} transients whereas astrocyte soma rarely showed spontaneous Ca^{2+} oscillations similar to previous reports using GECIs. We exploited this new approach to show these signals were independent of neuronal spiking, metabotropic glutamate receptor (mGluR) activity, TRPA1 channels, and L- or T-type voltage-gated calcium channels. Removal of extracellular Ca^{2+} almost completely and reversibly abolished the spontaneous signals while IP_3R2 KO mice also exhibited spontaneous and compartmentalized signals, suggesting they rely on influx of extracellular Ca^{2+}. The Ca^{2+} influx dependency of the spontaneous signals in patch-loaded astrocytes was also observed in astrocytes expressing GCaMP3, further highlighting the presence of Ca^{2+} influx pathways in astrocytes. The mechanisms underlying these localized Ca^{2+} signals are critical for understanding how astrocytes regulate important functions in the adult brain.

GLIA 2016;64:2093–2103

Key words: two-photon, glia, microdomain, Fluo-4, Calcium Green-1 dextran, GCaMP, IP_3R2, TRPA1, synaptic, calcium channel

Introduction

Protoplasmic astrocytes in the grey matter create a network of highly complex fine processes that occupy a large volume and envelop neuronal synapses (Khakh and Sofroniew, 2015; Matyash and Kettenmann, 2010), even up to 2 million synapses each in the human cortex (Oberheim et al., 2006). The electrically inexcitable astrocyte both responds to neuronal activity and releases transmitters via intracellular Ca^{2+} elevations. A large body of evidence suggests Ca^{2+} elevations can be triggered by synaptically released glutamate acting on astrocyte G_q-linked mGluR5, leading to IP_3-dependent release of Ca^{2+} from internal stores (Araque et al., 2014; Volterra et al., 2014). However, the functional roles of astrocyte Ca^{2+} elevations were recently challenged based on a lack of observable phenotypes in mice lacking the astrocyte specific IP_3R isoform (IP_3R2) (Agulhon et al., 2010; Bonder and McCarthy, 2014; Fiacco et al., 2007; Nizar et al., 2013). Additionally, mGluR5s receptors are developmentally down regulated in astrocytes of the adult (Sun et al., 2013). However, these studies mainly examined Ca^{2+} signaling in the astrocyte somata due to limitations of conventional dye loading techniques. Astrocytes form fine networks of processes that densely cover specified non-overlapping domains and the mechanisms underlying Ca^{2+} responses in these fine processes that surround and enwrap synaptic structures may be different from but equally important to somatic responses.

View this article online at wileyonlinelibrary.com. DOI: 10.1002/glia.23042

Published online August 1, 2016 in Wiley Online Library (wileyonlinelibrary.com). Received Mar 14, 2016, Accepted for publication July 13, 2016.

Address correspondence to: Brian MacVicar, Djavad Mowafaghian Centre for Brain Health, University of British Columbia, Vancouver, BC V6T 2B5, Canada. E-mail: bmacvicar@brain.ubc.ca

From the Djavad Mowafaghian Centre for Brain Health, University of British Columbia, Vancouver, BC, V6T 2B5, Canada

Additional Supporting Information may be found in the online version of this article.

Additionally, given the vast transcriptional and protein expression profile of multiple channels, transporters and receptors in astrocytes (Holtman et al., 2015; Sharma et al., 2015; Zhang et al., 2014), intracellular Ca^{2+} fluctuations are likely governed by multiple signaling pathways. These findings raise the question of how Ca^{2+} levels are regulated in adult mouse astrocytes, particularly in the fine processes that oppose synaptic structures.

The specific expression of GECIs in astrocytes was first shown by Shigetomi et al., to reveal Ca^{2+} signals in compartments that were not visible with organic dyes and bulk loading (Shigetomi et al., 2010). Recently the expression of GECIs in astrocytes has revealed that new levels of complexity occur in the fine and distal processes of the astrocytes that are not reflected in the soma both *in vitro* and *in vivo* (Kanemaru et al., 2014; Otsu et al., 2015; Shigetomi et al., 2013a; Shigetomi et al., 2013b; Srinivasan et al., 2015; Zhang et al., 2014). Surprisingly, these fine process Ca^{2+} signals have been shown to occur spontaneously in the absence of neuronal spiking and to persist even when the IP_3R2 gene is deleted (Haustein et al., 2014; Kanemaru et al., 2014; Srinivasan et al., 2015). However, there are concerns that chronic expression of GECIs may modify astrocyte Ca^{2+} signaling via homeostatic mechanisms from enhanced Ca^{2+} buffering by the GECI itself. Additionally the transfection methods often used to express GECIs may have adverse effects on astrocyte function (Ortinski et al., 2010; Volterra et al., 2014). The large body of literature studying astrocyte calcium with bulk loading techniques has been predominantly focused on G_q-linked responses, requiring IP_3-dependent release from internal stores (Araque et al., 2014). Even when patch clamping single astrocytes *in situ* in order to analyze signals from astrocyte processes, only G_q-linked responses were observed (Di Castro et al., 2011; Panatier et al., 2011). In order to resolve these issues, we developed new methods to image astrocyte Ca^{2+} using fluorescent indicators within the entire domain of a single astrocyte. This approach allowed us to evaluate the contribution of Ca^{2+} entry or release from IP_3 mediated stores in transgenic mice where putative candidate Ca^{2+} entry channels such as voltage-gated Ca^{2+} channels (Cheli et al., 2016; Latour et al., 2003) or TRPA1 channels (Shigetomi et al., 2012) were knocked out. Our results point to a yet undescribed calcium entry pathway underlying the Ca^{2+} transients in the fine processes of astrocytes.

Materials and Methods

Mice

Postnatal day p45–120 mice (female and male) were used for all experiments. Experiments were conducted between 1 and 10 hours following the start of the light cycle. Mice came from following sources: C57BL/6 WT mice, Charles River Laboratories; $IP_3R2^{-/-}$, Dr. Ju Chen, UCSD (Li et al., 2005); $TRPA1^{-/-}$, Jackson Laboratories (Kwan et al., 2006); $Ca_v1.3^{-/-}$, (Dr. Striessnig, University of Innsbruck via Dr. Surmeier at Northwestern University) (Platzer et al., 2000). SLC1a3(GLAST)-cre/ERT mice and (Ai38)ROSA26-LSL-GCaMP3 from Jackson Laboratories were crossed to produce mice expressing GCaMP3 in astrocytes when administered tamoxifen, as previously described (Paukert et al., 2014). Three doses of 4 mg tamoxifen were injected IP at 48 hour intervals 1–2 weeks prior to experiments.

Abbreviations

CBX Carbenoxolone
PE Phenylephrine

Slice Preparation

Brain slices were prepared as previously described (Rungta et al., 2015), according to protocols approved by the University of British Columbia Committee on Animal Care. Brains were rapidly extracted and placed into ice-cold slicing solution containing (in mM): NMDG, 120; KCl, 2.5; $NaHCO_3$, 25; $CaCl_2$, 1; $MgCl_2$, 7; NaH_2PO_4, 1.25; glucose, 20; Na-pyruvate, 2.4; and Na-ascorbate, 1.3; saturated with 95% O_2/5% CO_2. Transverse hippocampal slices, 300 μm thick, were sliced using a vibrating tissue slicer (VT1200, Leica, Nussloch, Germany). Slices were incubated at 32°C in artificial CSF containing (in mM): NaCl, 126; KCl, 2.5; $NaHCO_3$, 26; $CaCl_2$, 2.0; $MgCl_2$, 1.5; NaH_2PO_4, 1.25; and glucose, 10; saturated with 95% O_2/5% CO_2 for 30 minutes. For experiments, slices were at 22–24°C and perfused at 2 mL/minute.

Dye Loading Protocol

Slices were first incubated in ACSF plus SR101 (1 μM) (Sigma, St. Lous, MO) at room temperature for 30 minutes. Astrocytes (65-100μm below the surface of the slice) were identified by SR101 positive staining and targeted for patch clamping using DIC optics. Astrocytes were voltage clamped at −80 mV with an intracellular solution containing the following (in mM) in addition to the Ca^{2+} indicator described below: 124 potassium gluconate, 4 $MgCl_2$, 10 HEPES, 4 potassium-ATP, 0.4 sodium-GTP, 10 Na_2 creatine PO_4, pH adjusted to 7.2, with KOH and osmolarity adjusted to 290–300 mOsm. Carbenoxolone (CBX; 40 μM) was perfused onto slices >10min before whole-cell configuration. All astrocytes with holding current >150pA were discarded. The dye was filled for 15-30 minutes following breakthrough to allow high signal to noise imaging of fine processes. In the majority of astrocytes, and for the analysis of all experiments in which comparisons were made between different mouse strains (transgenic vs. wild-type), the patch pipette was withdrawn from the slice prior to imaging. Additionally, when mouse strains were compared all experiments within the two groups were acquired on the same setup by the same experimenter. In astrocytes from adult brain slices we found that the membrane would reseal on its own in the majority of patched astrocytes within 30 minutes. This facilitated removal of the patch pipette without damaging the cell. During the pipette withdrawal the astrocyte was imaged live in frame scan mode and any cells that exhibited a large increase in somatic Ca^{2+} were discarded. The following dyes (Invitrogen, Carlsbad, CA) were included in the patch pipette during separate experiments, Fluo-4 potassium salt (200 μM) or Calcium Green-1 dextran, potassium salt (3000 MW).

Pharmacology

Drugs were purchased from the following suppliers; carbenoxolone, tACPD, (Sigma, St. Louis, MO); HC030031, MPEP, CPCCOEt, nimodipine, phenylephrine (Tocris, Bristol, UK). Z944 was a gift from Dr. Terrance Snutch (University of British Columbia). All drugs were bath applied.

Imaging

Imaging was performed with a two-photon laser-scanning microscope (Zeiss LSM510 Meta NLO or LSM7MP; Zeiss, Oberkochen, Germany) with a 40X-W/1.0NA or 20X-W/1.0NA objective lens directly coupled to a Chameleon Ultra2 laser (Coherent, Santa Clara, CA). Fluo-4 and Calcium Green dyes were excited at 810 nm and GCaMP3 was excited at 920 nm. The fluorescence emission was split using a dichroic mirror at 560 nm, and the signals were each detected with photo multiplier tubes after passing through appropriate emission filters (SR101: 605 nm, 55 nm band pass; Fluo-4, Calcium Green, GCaMP3: 525 nm, 50 nm band pass). Frame scanning mode was performed at a frequency of 0.13-0.26 Hz.

Data Collection, Analysis, and Statistics

Translational movement in the XY plane was removed using Image J software. Fluorescence signals were defined as delta F/F (dF/F) = $[((F_1 - B_1)-(F_0 - B_0))/(F_0 - B_0)]$, where F_1 and F_0 are fluorescence at a given time and mean F in the absence of events, respectively. B_1 and B_0 are the corresponding background fluorescence signals. 12-20 ROIs were selected from each cell. ROIs had a dimension of 2 μm × 2 μm as this encompassed the pixels that usually constituted an active region. ROIs were chosen that were >4 μm from the nearest ROI. The size of the ROI was chosen to measure microdomain signals within the meshwork of fine processes rather than Ca^{2+} transients in single processes. To ensure F_0 accurately represented the resting Ca^{2+} level between Ca^{2+} transients we iteratively excluded the larger transients from the computation of F_0 until the resulting mean changed by <1%. Events were defined as starting when F > 3 SD and ending when F < 3SD from the computed F_0. Experimental values are the mean ± SEM; baseline equals 100%. *n* values used for statistical comparisons represent the number of experiments. The mean values for event frequency and amplitude from each experiment were used to represent each *n*. Statistical tests were done with a two-tailed Student's *t*-test $P < 0.05$ was accepted as statistically significant ($^*P < 0.05$, $^{**}P < 0.01$, $^{***}P < 0.001$).

Results

Imaging Ca^{2+} Signals Within the Entire Domain of a Single Adult Astrocyte Using Fluorescent Dyes

We tested whether restricting the diffusion of a cytoplasmic Ca^{2+} indicator dye to a single astrocyte with two independent approaches would provide a sufficient signal to noise ratio to allow us to resolve the network of fine and distal processes. Dye loading via patch pipettes can provide high signal to noise signals in neuronal distal dendrites and spines but is problematic in astrocytes because dyes readily diffuse into adjacent astrocytes via gap junctions (Dissing-Olesen et al., 2014; Gutnick et al., 1981). We either patch-loaded astrocytes with the dextran conjugated Ca^{2+} indicator, Calcium Green-1 dextran (3000MW), that was too large (>1kDa) to diffuse across gap junctions or we combined whole-cell dialysis of astrocytes with the Ca^{2+} indicator Fluo-4 while simultaneously blocking gap junctions. Individual astrocytes stained with SR101 were targeted for patch-loading with calcium indicator dye. If Fluo-4 was in the pipette, the gap junction blocker carbenoxelone (40μM) was perfused onto the slice prior to entering whole cell configuration. In the presence of the gap junction blocker, we observed that the high-affinity Ca^{2+} indicator Fluo-4 dialzyzed throughout the fine processes of the cell but remained restricted to a single astrocyte when compared to the SR101 staining (Fig. 1A). Dialysis of Calcium Green-1 dextran (3000MW) in the absence of carbenoxolone, resulted in identical dye-filling patterns of single astrocytes and their processes, showing dye restriction within single cells (Fig. 1B). The z-stack projection (Fig. 1A) of the astrocyte shows the dense mesh of fine processes not observed by staining astrocytes with SR101. Frame scanning of astrocytes under these conditions revealed compartmentalized Ca^{2+} elevations that were restricted to regions in the fine, distal processes and were not reflected in soma signals (Fig. 1C,D and Supp. Info. Movie 1). When similar imaging experiments were conducted without carbenoxolone using Calcium Green-1 dextran we observed an identical pattern of spontaneous compartmentalized Ca^{2+} elevations in fine processes (but not soma) as seen by comparing results obtained with either Fluo-4 and or Calcium Green-1 dextran (Fig. 1D–F). This demonstrates that carbenoxolone does not alter these spontaneous, discrete Ca^{2+} signals and indicates that these compartmentalized Ca^{2+} signals in fine process do not depend on gap junction proteins. These two approaches of dialysis with different calcium indicator dyes to measure Ca^{2+} fluctuations within the entire domain of the astrocyte confirms the presence of microdomain Ca^{2+} signals that appear uncorrelated and independent from somatic activity.

Microdomain Ca^{2+} Signals Are Independent of Neuronal Spiking, Metabotropic Glutamate Group 1 Receptor Activation or TRPA1 Channels

We next took advantage of our Fluo-4 patch-loading protocol to examine the basis for these Ca^{2+} fluctuations in the fine processes of astrocytes without requiring cross-breeding or viral injections to obtain GECIs in transgenic mouse lines. In juvenile brains (younger than postnatal day 21) from mice or rats it is well established that glutamate released from neurons evokes intracellular Ca^{2+} elevations in astrocytes via the activation of mGluR group 1 receptors (Araque et al., 2014). However, recently it was shown that mGluR5 expression undergoes a developmental shift with low expression levels in adult mice

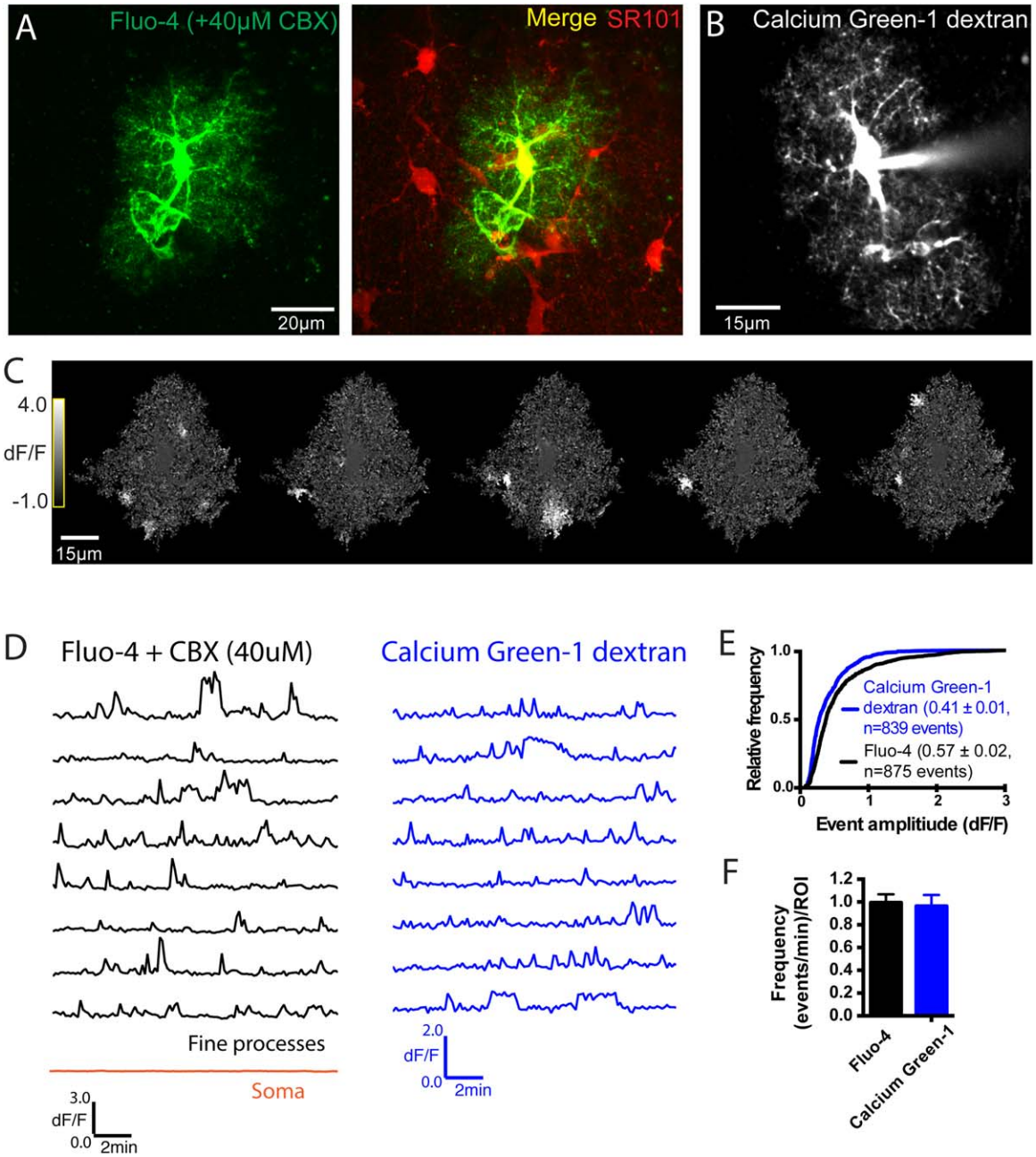

FIGURE 1: Spontaneous Ca^{2+} signaling observed in the fine processes of dye loaded astrocytes. (A) Maximum intensity projection in z (35μm) of an astrocyte filled with Fluo-4 (+40μM CBX in the external solution) among adjacent astrocytes bulk loaded with SR101 (B) Median intensity projection from a 60 frame time series of an astrocyte filled with Calcium Green-1 dextran (3000MW). (C) dF/F images of an astrocyte (Fluo-4) at different time points shows examples of astrocyte microdomain signaling. (D) Traces (dF/F) from ROIs of an astrocyte loaded with Fluo-4 + 40 μM CBX (left) or Calcium Green-1 dextran without CBX (right) shows uncorrelated spontaneous signaling that is independent of blocking gap junctions. (E) Cumulative frequency plot of event amplitude in Fluo-4 loaded (4 mice) and Calcium Green-1 dextran loaded (4 mice) astrocytes. Values in cumulative frequency plot represent mean ± SEM calculated using number of events. (F) Average frequency of events/min/ROI is similar in Calcium Green-1 dextran loaded and Fluo-4 loaded astrocytes.

(Sun et al., 2013) and no elevation of somatic Ca^{2+} was observed from activation mGluR group 1 receptors in astrocytes of adult mice and rats (Duffy and MacVicar, 1995; Sun et al., 2013). Given the results that spontaneous fine process Ca^{2+} signals are not correlated with signals in the soma, it is possible that mGluR5 receptors are redistributed to more distal sites in the adult mouse. We first tested whether blocking neuronal spiking would alter the frequency or amplitude of the microdomain Ca^{2+} signals, as has been observed with Fluo-4 in the thicker primary and secondary branches of astrocytes in the dentate gyrus (Di Castro et al., 2011) and in CA1 of the young rat (Panatier et al., 2011). Surprisingly, in the fine

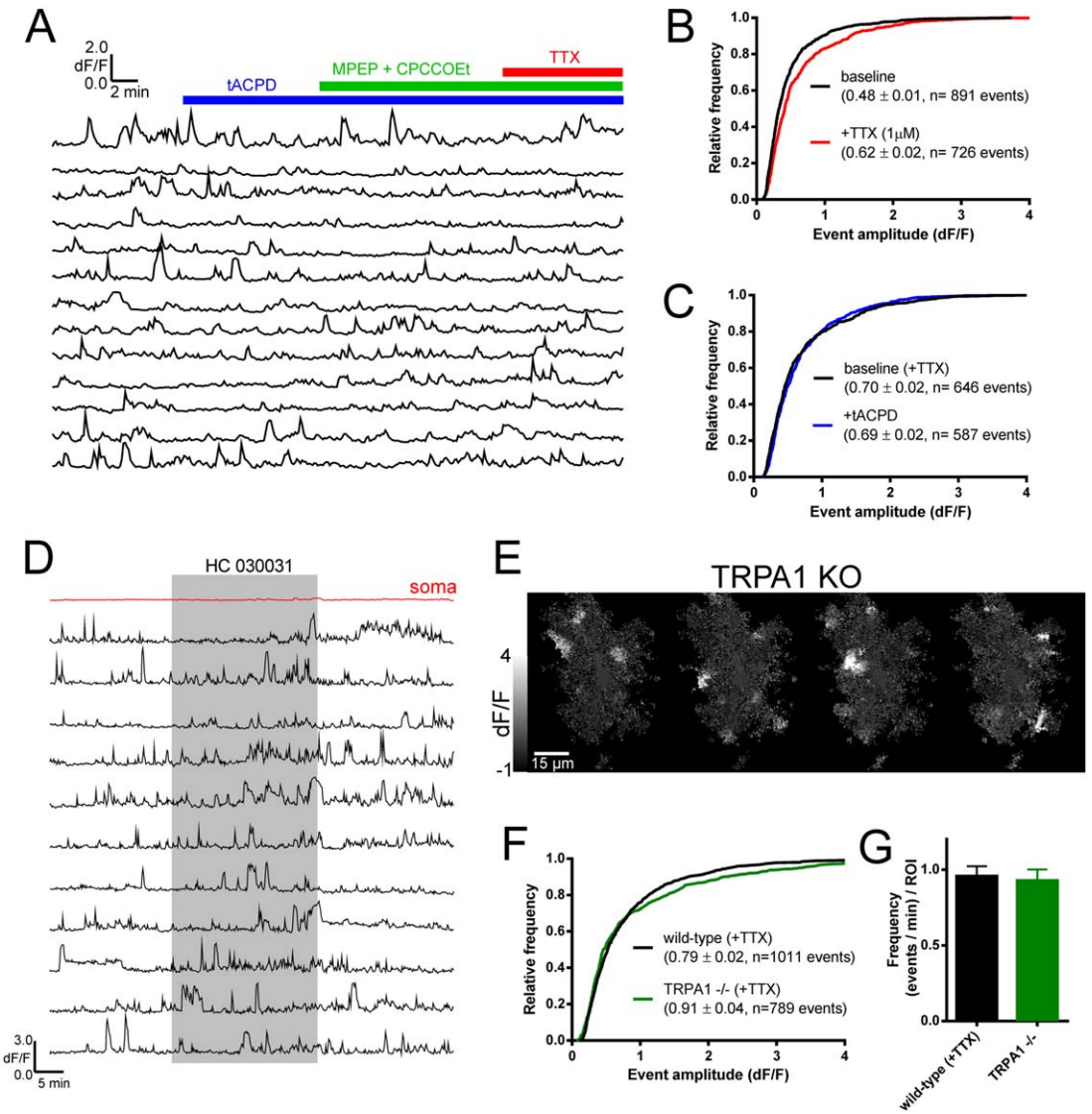

FIGURE 2: Pharmacological analyses of fine process Ca^{2+} signaling. (A) Traces from ROIs of an astrocyte in which tACPD (50 μM) was applied to activate mGluR group 1 followed by MPEP (10μM) and CPCCOEt (100 μM) to block mGluR5 and 1 respectively. TTX (1 μM) was applied at end of trace to test contribution of neuronal spiking. (B) Cumulative frequency plot showing that blocking neuronal spiking with TTX did not reduce the amplitude of spontaneous Ca^{2+} signals compared to baseline (no blockers) conditions (4 mice). (C) Cumulative frequency plot shows no effect on amplitude of Ca^{2+} signals when activating mGluR group 1 with 50 μM tACPD in TTX solution (4 mice). (D) Traces from ROIs of a Fluo-4 loaded astrocyte showing that application of HC 030031 (80 μM) has no effect on spontaneous events in TTX (E) dF/F images of a Fluo-4 loaded astrocyte from TRPA1$^{-/-}$ mouse at various time points F) Cumulative frequency plot shows similar distribution in wild-type and TRPA1$^{-/-}$ mice in TTX solution (control, 6 mice; TRPA1$^{-/-}$, 5 mice). (G) Similar frequency of spontaneous events observed in wild-type and TRPA1$^{-/-}$ mice. Values in cumulative frequency plots represent mean ± SEM calculated using number of events. Data from wild-type mice in F and G is replotted in Fig. 4.

processes of adult mouse CA1 astrocytes we observed no significant reduction in either the mean amplitude (133.8 ± 16.4% from baseline, $n = 4$, $P > 0.05$) or frequency (84.7 ± 5.2%, $n = 4$, $P > 0.05$) of spontaneous events when neuronal spiking was blocked with TTX (1 μM; Fig. 2A,B). This is in agreement with results obtained from imaging GCaMP3 in CA3 astrocytes, which revealed that TTX had no significant effect on spontaneous transients in either the somata or branches throughout the entire domain of the astrocyte (Haustein et al., 2014). Additionally, application of tACPD (50 μM) to activate mGluR group 1 did not trigger Ca^{2+} elevations in either fine processes or somata, nor did it significantly affect the frequency (89.8 ± 6.1%, $n = 4$, $P > 0.05$) or amplitude (97.2 ± 4.2%, $n = 4$, $P > 0.05$) of the spontaneous events when added in the presence of TTX to minimize neuronal activation (Fig. 2A,C).

TRPA1 channels are non-selective cation channels permeable to Ca^{2+} that have been reported to mediate a major proportion of spontaneous near-membrane Ca^{2+} signals in

both primary astrocytes and organotypic slice culture preparations imaged with membrane-tethered Ca^{2+} indicators (Jackson and Robinson, 2015; Shigetomi et al., 2012). In the CA1 area of acute hippocampal slices, blocking TRPA1 with HC 030031 only reduced the frequency of near-membrane Ca^{2+} signals by ~20% (Shigetomi et al., 2013b). In contrast, HC030031, had no effect on the frequency of spontaneous Ca^{2+} signals in CA3 astrocytes imaged with the cytosolic GECI, GCaMP3(Haustein et al., 2014). This discrepancy might be due to either heterogeneity of CA3 and CA1 astrocytes or failure of cytosolic GCaMP3 to detect the near-membrane TRPA1 signals. In our experiments using Fluo-4 to image fine processes, we observed no significant effect of the TRPA1 antagonist HC 030031 on frequency ($109.3 \pm 14.6\%$, $n = 3$, $P > 0.05$) or amplitude ($103.4 \pm 7.4\%$, $n = 3$, $P > 0.05$) of events (Fig. 2D). Additionally, astrocytes loaded with Fluo-4 in slices from TRPA1$^{-/-}$ mice still displayed robust and frequent Ca^{2+} transients in the fine processes (Fig. 2E–G). These results are consistent with observations that the cytosolic GECIs fail to resolve all near-membrane signals observed with membrane-tethered GECIs (Shigetomi et al., 2010), as only a minor proportion of near-membrane Ca^{2+} signals are mediated by TRPA1 in CA1 astrocytes from hippocampal slices (Shigetomi et al., 2013b). Our method of loading Fluo-4 into the fine processes allows us to sample cytoplasmic signals that may overlap with those strictly localized near the plasma membrane that are only observed with membrane-tethered indicators.

Spontaneous Fine Process Microdomain Ca^{2+} Elevations Are Mediated by Ca^{2+} Influx and Persist in IP_3R2 KO Mice

It is important to understand whether the elevations of intracellular Ca^{2+} that occur in the fine processes occur via IP_3R-dependent pathways, as is the case for a large proportion of the signaling observed in the astrocyte somata and thicker processes (Volterra et al., 2014). We found that within 5 minutes, removal of extracellular Ca^{2+} reversibly eliminated transients in fine processes in both Fluo-4 loaded and GCaMP3 expressing astrocytes (Fig. 3A–D). We confirmed that the effect was not due to depletion of intracellular stores as activation of the G_q-coupled $\alpha 1$ adrenoreceptors with phenylephrine (PE) after extracellular Ca^{2+} was depleted, triggered a large amplitude global elevation in both fine processes and the soma (Fig. 3B,E,F). This suggests that spontaneous microdomain Ca^{2+} signals occur via an unidentified transmembrane channel or transporter. Additionally, we observed that the resting Ca^{2+} (F_0) of the astrocyte in the absence of transients, was also reversibly decreased upon removal of extracellular Ca^{2+} ($57.5 \pm 14.1\%$ of baseline in Ca^{2+} free vs. $101.5 \pm 15.5\%$ after washout, $n = 4$, $P < 0.01$, Fig. 3A), suggesting that the microdomain Ca^{2+} transients help regulate basal Ca^{2+} levels in the astrocyte. To further confirm that these signals did not require activation of IP_3Rs, we patch-loaded astrocytes from $IP_3R2^{-/-}$ mice, in which the predominant isoform of the IP_3R in astrocytes is deleted. The $IP_3R2^{-/-}$ mouse has often been used to conclusively demonstrate roles or lack thereof for astrocyte Ca^{2+} in several physiological processes without ensuring Ca^{2+} signals are completely eliminated (Agulhon et al., 2010; Bonder and McCarthy, 2014; Fiacco et al., 2007; Nizar et al., 2013). We confirmed that IP_3R2 deletion abolished G_q-mediated signals, as PE failed to induce Ca^{2+} elevations in astrocytes from these mice ($n = 4$ mice). However, even though G_q-mediated responses were abolished, spontaneous activity in the fine processes was still largely observed in IP_3R2 KO mice (Fig. 3G–I). Taken together these results suggest that the majority of the observed spontaneous fine process Ca^{2+} signals involved a Ca^{2+} influx pathway, similar to results obtained with GECIs.

Spontaneous Fine Process Ca^{2+} Influx Is Not Mediated by Activation of L- or T-Type voltage-Gated Calcium Signals

Among the possible candidates of a transmembrane Ca^{2+} influx pathway in astrocytes are subtypes of voltage-gated calcium channels (VGCCs) that were first reported in astrocytes in cell culture (Barres et al., 1989; MacVicar, 1984). Although expression of voltage-gated calcium channels in astrocytes *in vivo* is low compared to neurons, transcriptome analysis of cortical astrocytes shows expression of *Cacna1d* ($Ca_v1.3$) and *Cacna1h* ($Ca_v3.2$) mRNA (Zhang et al., 2014). L-type VGCCs are expressed in cultured astrocytes (D'Ascenzo et al., 2004; Latour et al., 2003), and have been shown to be upregulated in reactive astrocytes following brain injury (Westenbroek et al., 1998) and surrounding amyloid-β plaques in mouse models of Alzheimer's dissease (Willis et al., 2010) *in vivo*. Recently astrocyte L-type VGCCs have been implicated in regulating the heterogeneity of presynaptic strengths at hippocampal pyramidal cell inputs in more physiological conditions (Letellier et al., 2016). We therefore tested the possibility that $Ca_v1.3$ channels mediated the fine process spontaneous calcium transients we observed, by loading Fluo-4 into astrocytes of $Ca_v1.3$ KO mice. Compared to astrocytes from wild-type mice, we did not observe a reduction in either amplitude or frequency of these events (Fig. 4A,B), suggesting that $Ca_v1.3$ channels are not a major player in the generation of these spontaneous signals. Additionally, to rule out a possible compensation by $Ca_v1.2$ channels, we perfused the L-type blocker nimodipine (20μM) onto slices of $Ca_v1.3$ KO mice, and recorded no significant reduction in the amplitude ($109.6 \pm 8.4\%$, $n = 4$, $P > 0.05$) or frequency ($94.3 \pm 5.9\%$, $n = 4$, $P > 0.05$) of spontaneous events (Fig. 4A,B). T-type

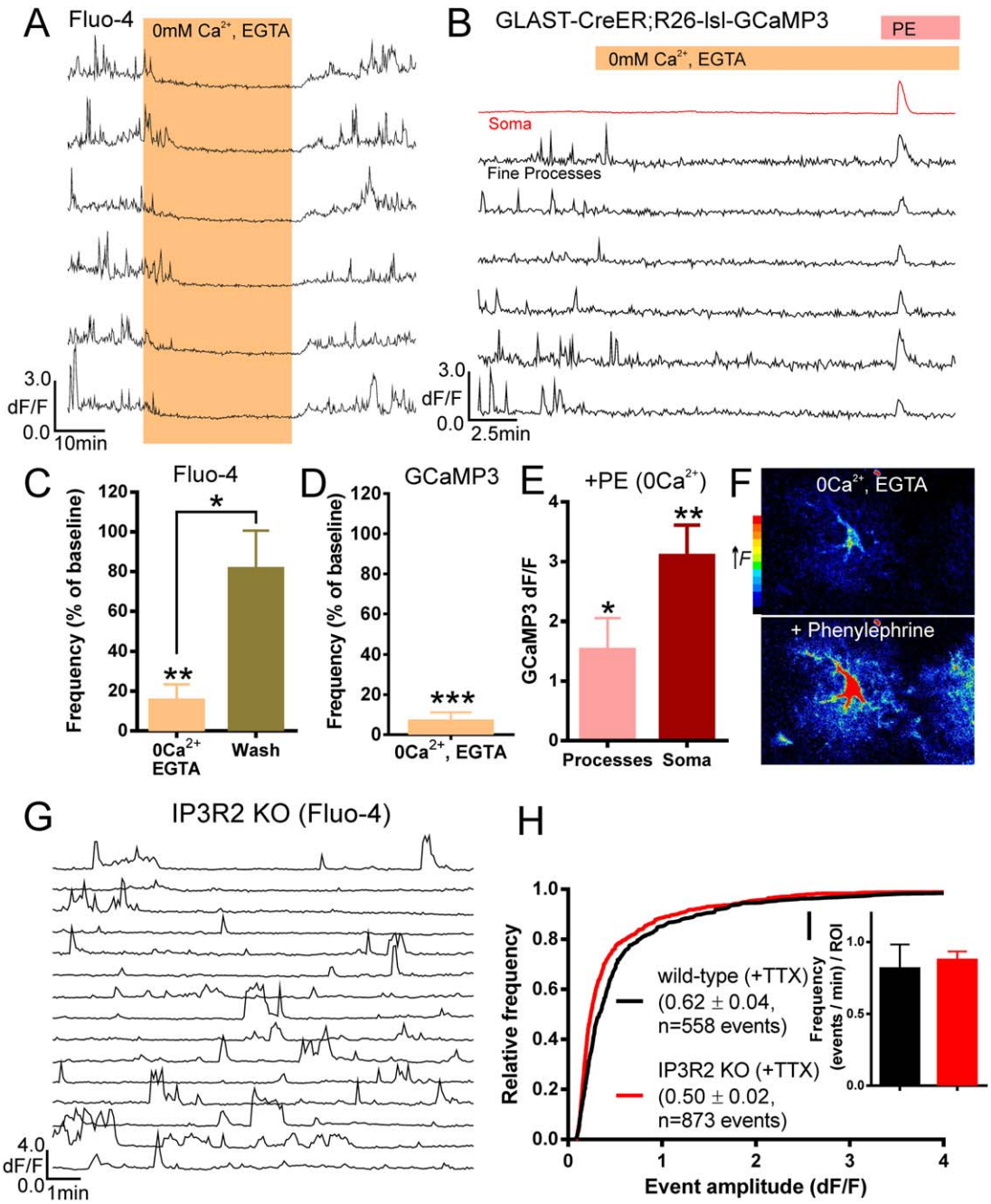

FIGURE 3: Spontaneous fine process Ca^{2+} signals are primarily mediated by transmembrane Ca^{2+} influx and independent of IP_3R2. (A) Spontaneous Ca^{2+} signals were dramatically reduced in fine processes of a Fluo-4 loaded astrocyte when perfused with 0mM Ca^{2+} + 2mM EGTA (Ca^{2+} chelator) external solution. (B) Ca^{2+}-free solution reduced spontaneous Ca^{2+} signals in fine processes of astrocytes expressing GCaMP3. The positive control at the end of the traces shows that application of phenylephrine (50 μM) still elicited a global calcium increase in the soma and throughout the processes indicating that ER stores were not depleted. (C) Frequency of spontaneous events is reversibly eliminated in Ca^{2+}-free external solution (n=4 mice). (D) Decrease in frequency of spontaneous Ca^{2+} signals in GCaMP3-expressing astrocytes (n=6 slices). (E, F) Phenylephrine (50 μM) caused large global increases in cytosolic Ca^{2+} in Ca^{2+}-free solution demonstrating internal stores were not Ca^{2+} depleted. (G) Traces from ROIs of a Fluo-4 loaded $IP_3R2^{-/-}$ astrocyte showing spontaneous Ca^{2+} transients still occurred in distal processes (in TTX). (H) Cumulative frequency plot of mean amplitude (wild-type, 4 mice; $IP_3R2^{-/-}$, 6 mice) and (I) histogram of event frequency shows that spontaneous Ca^{2+} elevations in distal processes of $IP_3R2^{-/-}$ and wild-type mice had similar properties. Values in cumulative frequency plot represent mean ± SEM calculated using number of events.

calcium channels are low-voltage activated calcium channels, which makes them an appealing candidate for fine process Ca^{2+} influx due to the highly negative resting potential of astrocytes. In order to test the contribution of $Ca_v3.2$ channels we perfused on the T-type VGCC blocker, Z944 (10μM) (Tringham et al., 2012). We observed no significant

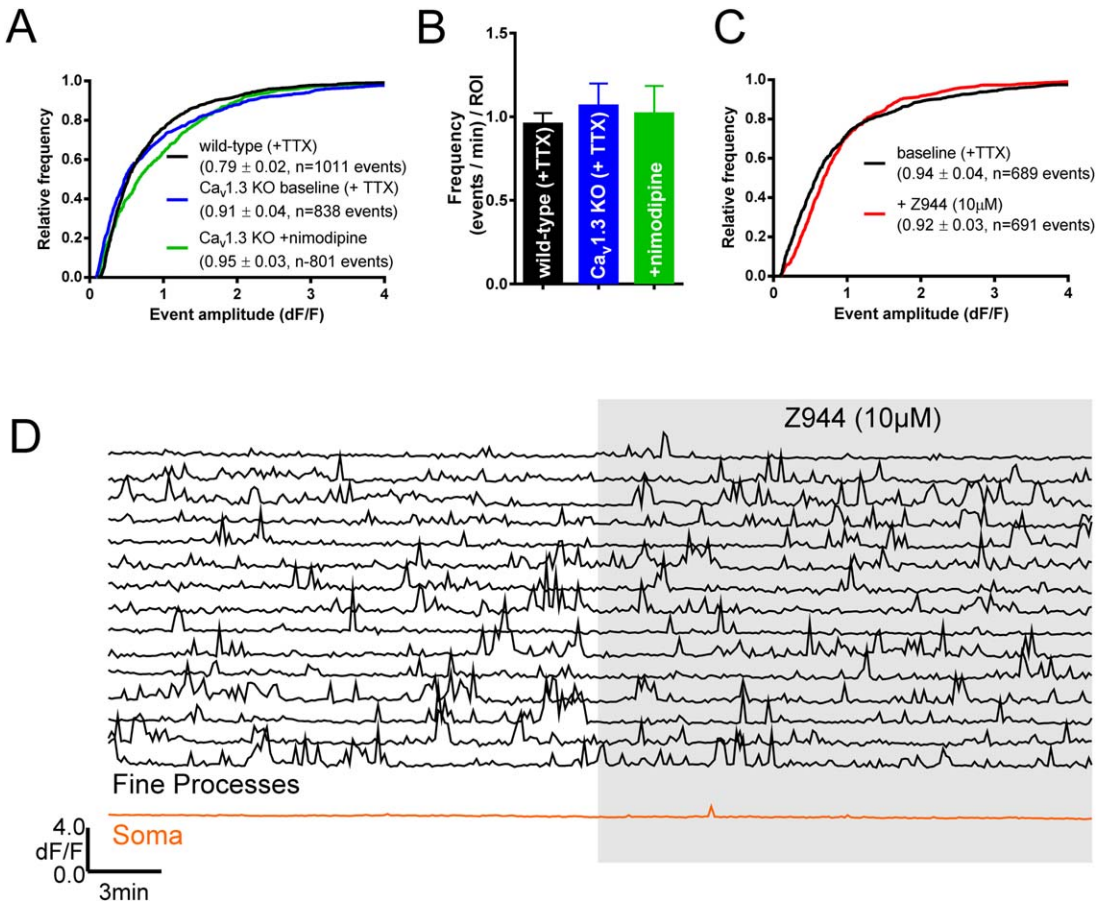

FIGURE 4: Spontaneous fine process Ca^{2+} signals are not mediated by L- or T-type voltage-gated calcium channels. (A) No reduction in amplitude of spontaneous events measured in astrocytes from Cav1.3 KO mice compared to wild-type mice in TTX solution (wild-type, 6 mice; $Ca_v1.3^{-/-}$, 4 mice). Application of nimodipine (20 μM) to slices from $Ca_v1.3$ KO mice does not reduce the amplitude of events. (B) Similar frequency of spontaneous events observed in astrocytes from wild-type and $Ca_v1.3^{-/-}$ mice, with no effect of nimodipine on the frequency of events in $Ca_v1.3^{-/-}$ mice. (C) Cumulative frequency plot showing that blocking T-type calcium channels with Z944 (10 μM) did not reduce the amplitude of spontaneous Ca^{2+} signals compared to baseline (in TTX) conditions (6 mice). (D) Traces from ROIs of a Fluo-4 loaded astrocyte showing that application of Z944 (10 μM, 200 fold greater than the IC_{50}) has no effect on spontaneous events (in TTX). Values in cumulative frequency plots represent mean ± SEM calculated using number of events. Same data from wild-type mice in A and B is also plotted in Fig. 2.

change in amplitude (112.7 ± 11.4%, $n = 6$, $P > 0.05$) or frequency (102.0 ± 14.8%, $n = 6$, $P > 0.05$) of events in the presence of Z944 (Fig. 4C,D), suggesting that the spontaneous events were neither mediated by $Ca_v3.2$ nor other T-type VGCCs. These results suggest that although VGCCs may contribute to astrocyte Ca^{2+} influx in response to sufficient membrane depolarization or during pathological conditions, the spontaneous events described here are not mediated by L- or T- type VGCCs.

Discussion

Our study describes Ca^{2+} dynamics in the fine processes of astrocytes using novel methods for obtaining high signal to noise responses without the need for expression of GECIs. The advantages of this technique over GECIs are that it does not require the generation of transgenic mice or viral transfection, does not induce long term homeostatic changes due to chronically buffering intracellular Ca^{2+} and that it is cost effective. Additionally, combining these techniques with the rapidly expanding library of transgenic mice allows for rapid screening of signaling mechanisms without the need for cross breeding. Furthermore, this method is not restricted to mice and permits examination of astrocyte fine process Ca^{2+} signaling in other rodents, non-human primates, and even human tissue. However, there are also concerns to patch-loading of indicator dyes such as intracellular disturbances due to dialysis. Although the use of carbenoxolone in the fluo-4 experiments might induce off-target effects, we did not observe changes in the frequency of astrocytic Ca^{2+} transients when compared to a Calcium Green-1 dextran dye that enabled observation of fine process Ca^{2+} dynamics without the need for gap junction blockers. Additionally, using

different technical approaches (patch-loading of fluorescent Ca^{2+} indicator dyes versus GECI expression) we observed similar properties of the Ca^{2+} transients in fine processes of astrocytes, suggesting that neither of the methods had significant impairments for detecting these signals.

Our results are largely in agreement with recent reports by other groups that used GECIs to describe spontaneous microdomain Ca^{2+} signals in the fine processes (Haustein et al., 2014; Kanemaru et al., 2014; Shigetomi et al., 2013a,b; Srinivasan et al., 2015; Zhang et al., 2014). We show that they are not dependent on neuronal action potentials or mGluR group 1 activation. Additionally, we demonstrated that these Ca^{2+} signals depend primarily on transmembrane Ca^{2+} influx as they were rapidly abolished when Ca^{2+} was removed from the external solution. Finally, we used an IP_3R2 KO mouse to verify that Ca^{2+} signals still occurred when the astrocyte specific IP_3R2 subtype was deleted. Past studies using the IP_3R2 KO mice have concluded a lack of astrocyte Ca^{2+} involvement in various phenotypes, despite only measuring Ca^{2+} signals in the soma of the astrocyte or testing the contribution of other signaling pathways. The fact that astrocyte Ca^{2+} transients are still observed in $IP3R2^{-/-}$ mice demonstrates that in the adult mouse multiple mechanisms control astrocyte Ca^{2+} signaling and the conclusions of previous studies need to be re-evaluated. In addition the complex interplay between release from intracellular stores and influx via plasma membrane exchangers and/or channels has to be investigated and resolved using appropriately sensitive techniques for conclusions concerning the roles for astrocyte Ca^{2+}-dependent pathways to be valid.

The mechanism underlying the Ca^{2+} entry pathway remains unknown, although it is very possible that multiple channels or transporters are involved. It was previously reported that in CA1 astrocytes of hippocampal slices a small proportion of the Ca^{2+} entry ($\sim$20% of transients) monitored with the membrane-tethered GECI, Lck-GCaMP3 occur via TRPA1 channels (Shigetomi et al., 2013b). Although we observed no significant effect of blocking TRPA1 with HC 030031, a key difference in our methodology was the restriction of Fluo-4 to the cytosol vs. the membrane-tethered indicators used in previous studies showing TRPA1 mediated Ca^{2+} transients. It has previously been shown that cytoplasmic GECIs failed to detect a proportion of near-membrane Ca^{2+} signals that were readily observed with membrane-tethered GECIs (Shigetomi et al., 2010), consistent with TRPA1 signals representing a subpopulation of signals that we failed to observe with cytoplasmic Fluo-4. Another study using cytosolic GCaMP3 also failed to detect any effect of blocking TRPA1 (Haustein et al., 2014), however these experiments were done in CA3 astrocytes that exhibit less near-membrane signals than CA1 astrocytes and may not express TRPA1. Interestingly, the largest effects of TRPA1 mediated Ca^{2+} signaling have been observed in primary cultures (Shigetomi et al., 2012) and organotypic slice cultures (Jackson and Robinson, 2015), suggesting that TRPA1 expression may be upregulated in reactive astrocytes. We also tested the possibility that L- or T-type VGCCs were underlying the spontaneous influx of Ca^{2+} in distal processes. Although electrophysiological analysis of such channels in neurons is feasible, it is technically difficult to analyze such conductances in the distal processes of mature astrocytes due to the poor space clamp arising from a very low membrane resistance (Zhou et al., 2009). Using our Ca^{2+} indicator approach we did not observe any contribution of VGCCs towards the generation of spontaneous events in distal processes. However, it remains an interesting but unresolved question of whether VGCCs may modify astrocyte Ca^{2+} signaling in reactive astrocytes following brain injury or in neurological diseases. L-type channel expression has been shown to be upregulated in reactive astrocytes following brain injury, hypomyelination, ischemia and surrounding amyloid-β plaques (Westenbroek et al., 1998; Willis et al., 2010), and astrocyte Ca^{2+} signaling has been shown to be altered surrounding amyloid-β plaques in a mouse models of Alzheimer's disease (Delekate et al., 2014; Kuchibhotla et al., 2009).

Elucidating the functional significance of these microdomain Ca^{2+} signals will be a major step in understanding astrocyte physiology. Of note, in addition to abolishing the spontaneous Ca^{2+} transients, the resting Ca^{2+} (F_0) of the astrocyte was also reversibly decreased upon removal of extracellular Ca^{2+}, supporting the view that the spontaneous influx of Ca^{2+} transients in microdomains regulates basal calcium levels in the astrocyte. An important function of spontaneous microdomain Ca^{2+} transients may be to regulate basal astrocyte Ca^{2+} levels which are important for the regulation of synaptic activity (Shigetomi et al., 2012) and resting arteriole diameter (Rosenegger et al., 2015). In hippocampal slice cultures, fine process Ca^{2+} has recently been shown to alter mitochondrial trafficking in an activity dependent manner, suggesting a possible interaction between Ca^{2+} elevations and local energy supply (Jackson and Robinson, 2015; Stephen et al., 2015), and *in vivo* Ca^{2+} elevations were shown to occur in fine processes but not the soma of olfactory glomeruli astrocytes in response to sensory stimulation (Otsu et al., 2015). Whether and how spontaneous fine process Ca^{2+} signals are related to and may be altered in response to synaptic activation as well as how this signaling may be altered in disease remain intriguing questions.

References

Agulhon C, Fiacco TA, McCarthy KD. 2010. Hippocampal short- and long-term plasticity are not modulated by astrocyte Ca2+ signaling. Science 327: 1250–1254.

Araque A, Carmignoto G, Haydon PG, Oliet SH, Robitaille R, Volterra A. 2014. Gliotransmitters travel in time and space. Neuron 81:728–739.

Barres BA, Chun LL, Corey DP. 1989. Calcium current in cortical astrocytes: Induction by cAMP and neurotransmitters and permissive effect of serum factors. J Neurosci 9:3169–175.

Bonder DE, McCarthy KD. 2014. Astrocytic Gq-GPCR-linked IP3R-dependent Ca2+ signaling does not mediate neurovascular coupling in mouse visual cortex in vivo. J Neurosci 34:13139–13150.

Cheli VT, Santiago Gonzalez DA, Smith J, Spreuer V, Murphy GG, Paez PM. 2016. L-type voltage-operated calcium channels contribute to astrocyte activation in vitro. Glia 64:1396–1415.

D'Ascenzo M, Vairano M, Andreassi C, Navarra P, Azzena GB, Grassi C. 2004. Electrophysiological and molecular evidence of L-(Cav1), N- (Cav2.2), and R- (Cav2.3) type Ca2+ channels in rat cortical astrocytes. Glia 45:354–363.

Delekate A, Fuchtemeier M, Schumacher T, Ulbrich C, Foddis M, Petzold GC. 2014. Metabotropic P2Y1 receptor signalling mediates astrocytic hyperactivity in vivo in an Alzheimer's disease mouse model. Nat Commun 5:5422-

Di Castro MA, Chuquet J, Liaudet N, Bhaukaurally K, Santello M, Bouvier D, Tiret P, Volterra A. 2011. Local Ca2+ detection and modulation of synaptic release by astrocytes. Nat Neurosci 14:1276–1284.

Dissing-Olesen L, LeDue JM, Rungta RL, Hefendehl JK, Choi HB, MacVicar BA. 2014. Activation of neuronal NMDA receptors triggers transient ATP-mediated microglial process outgrowth. J Neurosci 34:10511–10527.

Duffy S, MacVicar BA. 1995. Adrenergic calcium signaling in astrocyte networks within the hippocampal slice. J Neurosci 15:5535–5550.

Fiacco TA, Agulhon C, Taves SR, Petravicz J, Casper KB, Dong X, Chen J, McCarthy KD. 2007. Selective stimulation of astrocyte calcium in situ does not affect neuronal excitatory synaptic activity. Neuron. 54:611–626.

Gutnick MJ, Connors BW, Ransom BR. 1981. Dye-coupling between glial cells in the guinea pig neocortical slice. Brain Res 213:486–492.

Haustein MD, Kracun S, Lu XH, Shih T, Jackson-Weaver O, Tong X, Xu J, Yang XW, O'Dell TJ, Marvin JS, Ellisman MH, Bushong EA, Looger LL, Khakh BS. 2014. Conditions and constraints for astrocyte calcium signaling in the hippocampal mossy fiber pathway. Neuron 82:413–429.

Holtman IR, Noback M, Bijlsma M, Duong KN, van der Geest MA, Ketelaars PT, Brouwer N, Vainchtein ID, Eggen BJ, Boddeke HW. 2015. Glia Open Access Database (GOAD): A comprehensive gene expression encyclopedia of glia cells in health and disease. Glia. 63:1495–1506.

Jackson JG, Robinson MB. 2015. Reciprocal regulation of mitochondrial dynamics and calcium signaling in astrocyte processes. J Neurosci 35:15199–15213.

Kanemaru K, Sekiya H, Xu M, Satoh K, Kitajima N, Yoshida K, Okubo Y, Sasaki T, Moritoh S, Hasuwa H, Mimura M, Horikawa K, Matsui K, Nagai T, Iino M, Tanaka KF. 2014. In vivo visualization of subtle, transient, and local activity of astrocytes using an ultrasensitive Ca(2+) indicator. Cell Rep 8:311–318.

Khakh BS, Sofroniew MV. 2015. Diversity of astrocyte functions and phenotypes in neural circuits. Nat Neurosci 18:942–952.

Kuchibhotla KV, Lattarulo CR, Hyman BT, Bacskai BJ. 2009. Synchronous hyperactivity and intercellular calcium waves in astrocytes in Alzheimer mice. Science 323:1211–1215.

Kwan KY, Allchorne AJ, Vollrath MA, Christensen AP, Zhang DS, Woolf CJ, Corey DP. 2006. TRPA1 contributes to cold, mechanical, and chemical nociception but is not essential for hair-cell transduction. Neuron 50:277–289.

Latour I, Hamid J, Beedle AM, Zamponi GW, Macvicar BA. 2003. Expression of voltage-gated Ca2+ channel subtypes in cultured astrocytes. Glia 41:347–353.

Letellier M, Park YK, Chater TE, Chipman PH, Gautam SG, Oshima-Takago T, Goda Y. 2016. Astrocytes regulate heterogeneity of presynaptic strengths in hippocampal networks. Proc Natl Acad Sci U S A 113:E2685–E2694.

Li X, Zima AV, Sheikh F, Blatter LA, Chen J. 2005. Endothelin-1-induced arrhythmogenic Ca2+ signaling is abolished in atrial myocytes of inositol-1,4,5-trisphosphate(IP3)-receptor type 2-deficient mice. Circ Res 96:1274–1281.

MacVicar BA. 1984. Voltage-dependent calcium channels in glial cells. Science 226:1345–1347.

Matyash V, Kettenmann H. 2010. Heterogeneity in astrocyte morphology and physiology. Brain Res Rev 63:2–10.

Nizar K, Uhlirova H, Tian P, Saisan PA, Cheng Q, Reznichenko L, Weldy KL, Steed TC, Sridhar VB, MacDonald CL, Cui J, Gratiy SL, Sakadzic S, Boas DA, Beka TI, Einevoll GT, Chen J, Masliah E, Dale AM, Silva GA, Devor A. 2013. In vivo stimulus-induced vasodilation occurs without IP3 receptor activation and may precede astrocytic calcium increase. J Neurosci 33:8411–8422.

Oberheim NA, Wang X, Goldman S, Nedergaard M. 2006. Astrocytic complexity distinguishes the human brain. Trends Neurosci 29:547–553.

Ortinski PI, Dong J, Mungenast A, Yue C, Takano H, Watson DJ, Haydon PG, Coulter DA. 2010. Selective induction of astrocytic gliosis generates deficits in neuronal inhibition. Nat Neurosci 13:584–591.

Otsu Y, Couchman K, Lyons DG, Collot M, Agarwal A, Mallet JM, Pfrieger FW, Bergles DE, Charpak S. 2015. Calcium dynamics in astrocyte processes during neurovascular coupling. Nat Neurosci 18:210–218.

Panatier A, Vallee J, Haber M, Murai KK, Lacaille JC, Robitaille R. 2011. Astrocytes are endogenous regulators of basal transmission at central synapses. Cell 146:785–798.

Paukert M, Agarwal A, Cha J, Doze VA, Kang JU, Bergles DE. 2014. Norepinephrine controls astroglial responsiveness to local circuit activity. Neuron 82: 1263–1270.

Platzer J, Engel J, Schrott-Fischer A, Stephan K, Bova S, Chen H, Zheng H, Striessnig J. 2000. Congenital deafness and sinoatrial node dysfunction in mice lacking class D L-type Ca2+ channels. Cell 102:89–97.

Rosenegger DG, Tran CH, Wamsteeker Cusulin JI, Gordon GR. 2015. Tonic local brain blood flow control by astrocytes independent of phasic neurovascular coupling. J Neurosci 35:13463–13474.

Rungta RL, Choi HB, Tyson JR, Malik A, Dissing-Olesen L, Lin PJ, Cain SM, Cullis PR, Snutch TP, MacVicar BA. 2015. The cellular mechanisms of neuronal swelling underlying cytotoxic edema. Cell 161:610–621.

Sharma K, Schmitt S, Bergner CG, Tyanova S, Kannaiyan N, Manrique-Hoyos N, Kongi K, Cantuti L, Hanisch UK, Philips MA, Rossner MJ, Mann M, Simons M. 2015. Cell type- and brain region-resolved mouse brain proteome. Nat Neurosci 18:1819–1831.

Shigetomi E, Bushong EA, Haustein MD, Tong X, Jackson-Weaver O, Kracun S, Xu J, Sofroniew MV, Ellisman MH, Khakh BS. 2013a. Imaging calcium microdomains within entire astrocyte territories and endfeet with GCaMPs expressed using adeno-associated viruses. J Gen Physiol 141:633–647.

Shigetomi E, Jackson-Weaver O, Huckstepp RT, O'Dell TJ, Khakh BS. 2013b. TRPA1 channels are regulators of astrocyte basal calcium levels and long-term potentiation via constitutive D-serine release. J Neurosci 33:10143–10153.

Shigetomi E, Kracun S, Sofroniew MV, Khakh BS. 2010. A genetically targeted optical sensor to monitor calcium signals in astrocyte processes. Nat Neurosci 13:759–766.

Shigetomi E, Tong X, Kwan KY, Corey DP, Khakh BS. 2012. TRPA1 channels regulate astrocyte resting calcium and inhibitory synapse efficacy through GAT-3. Nat Neurosci 15:70–80.

Srinivasan R, Huang BS, Venugopal S, Johnston AD, Chai H, Zeng H, Golshani P, Khakh BS. 2015. Ca(2+) signaling in astrocytes from Ip3r2() mice in brain slices and during startle responses in vivo. Nat Neurosci 18:708–717.

Stephen TL, Higgs NF, Sheehan DF, Al Awabdh S, Lopez-Domenech G, Arancibia-Carcamo IL, Kittler JT. 2015. Miro1 regulates activity-driven positioning of mitochondria within astrocytic processes apposed to synapses to regulate intracellular calcium signaling. J Neurosci 35:15996–16011.

Sun W, McConnell E, Pare JF, Xu Q, Chen M, Peng W, Lovatt D, Han X, Smith Y, Nedergaard M. 2013. Glutamate-dependent neuroglial calcium signaling differs between young and adult brain. Science 339:197–200.

Tringham E, Powell KL, Cain SM, Kuplast K, Mezeyova J, Weerapura M, Eduljee C, Jiang X, Smith P, Morrison JL, Jones NC, Braine E, Rind G, Fee-Maki M, Parker D, Pajouhesh H, Parmar M, O'Brien TJ, Snutch TP. 2012. T-type calcium channel blockers that attenuate thalamic burst firing and suppress absence seizures. Sci Transl Med 4:121ra19-

Volterra A, Liaudet N, Savtchouk I. 2014. Astrocyte Ca(2)(+) signalling: An unexpected complexity. Nat Rev Neurosci 15:327–335.

Westenbroek RE, Bausch SB, Lin RC, Franck JE, Noebels JL, Catterall WA. 1998. Upregulation of L-type Ca2+ channels in reactive astrocytes after brain injury, hypomyelination, and ischemia. J Neurosci 18:2321–2334.

Willis M, Kaufmann WA, Wietzorrek G, Hutter-Paier B, Moosmang S, Humpel C, Hofmann F, Windisch M, Knaus HG, Marksteiner J. 2010. L-type calcium channel CaV 1.2 in transgenic mice overexpressing human AbetaPP751 with the London (V717I) and Swedish (K670M/N671L) mutations. J Alzheimers Dis 20:1167–1180.

Zhang Y, Chen K, Sloan SA, Bennett ML, Scholze AR, O'Keeffe S, Phatnani HP, Guarnieri P, Caneda C, Ruderisch N, Deng S, Liddelow SA, Zhang C, Daneman R, Maniatis T, Barres BA, Wu JQ. 2014. An RNA-sequencing transcriptome and splicing database of glia, neurons, and vascular cells of the cerebral cortex. J Neurosci 34:11929–11947.

Zhou M, Xu G, Xie M, Zhang X, Schools GP, Ma L, Kimelberg HK, Chen H. 2009. TWIK-1 and TREK-1 are potassium channels contributing significantly to astrocyte passive conductance in rat hippocampal slices. J Neurosci 29: 8551–8564.